INORGANIC SYNTHESIS
AND INDUSTRIAL INORGANIC CHEMISTRY

Influence of the Hydrothermal Synthesis Conditions on the Photocatalytic Activity of Titanium Dioxide Nanorods

T. M. Serikov[a],*, N. Kh. Ibrayev[a], T. M. Ivanova[b], and S. V. Savilov[b,c]

[a] Academician Buketov Karaganda University, ul. Universitetskaya 28, Karaganda, 10026 Kazakhstan
[b] Kurnakov Institute of General and Inorganic Chemistry, Russian Academy of Sciences, Moscow, 119991 Russia
[c] Faculty of Chemistry, Moscow State University, Moscow, 119991 Russia
*e-mail: serikov-timur@mail.ru

Abstract—Films of TiO_2 nanorods prepared under different conditions of hydrothermal synthesis were studied. With an increase in the hydrothermal synthesis temperature at a synthesis time of 24 h, the length of the TiO_2 nanorods formed first increases and then decreases, and the nanorod diameter changes. The TiO_2 film consisting of nanorods 4100 nm long and 100 nm in diameter, prepared at 180°C, exhibits the highest photocatalytic activity. This effect is predominantly associated with high specific surface area of the samples.

Keywords: titanium dioxide, nanorods, dye photodegradation, specific surface area

Owing to semiconductor properties, low toxicity, chemical stability, and relatively low cost, TiO_2-based nanomaterials are widely used as effective photocatalysts for wastewater treatment to remove toxic pollutants and for water decomposition to obtain gaseous hydrogen, and also as a material for dye-sensitized solar cells [1–3].

In the course of using films formed by TiO_2 nanoparticles, in which the electron transport occurs mainly over the nanoparticle surface, the heat treatment and sintering can lead to the formation of surface defects promoting recombination processes. To reduce the loss and prevent possible recombination processes in transition of charge carriers from one particle to another, it is promising to use nanostructures with 1D electron transport [4], such as TiO_2 nanotubes [5], nanorods [6], and nanothreads [7]. Among nanostructures, for titanium dioxide nanorods (TiO_2 NRs) it is possible to control the morphology and ensure high degree of ordering by varying the synthesis method. Hydrothermal method is the most feasible and the simplest method for preparing TiO_2 nanorods. It allows preparation of arrays of single crystalline TiO_2 nanorods of rutile modification on glass supports with a conducting fluorine-doped tin oxide (FTO) layer.

The synthesis time and heat treatment of TiO_2 nanorods prepared by hydrothermal synthesis can influence the photocatalytic activity of the films. High heat treatment temperature allows the crystal size to be increased, thus decreasing the amount of surface defects in the material, which leads to a decrease in the electron pair recombination rate and favors enhancement of the photocatalytic activity. Yamazaki et al. [8] reported that the photocatalytic activity of the nanorods increased with an increase in the nanorod annealing temperature from 400 to 800°C, despite a decrease in the specific surface area [8]. Depending on the hydrothermal synthesis time, the length of the nanorods formed varied in the interval 0.28–1.8 μm, which significantly influenced their photoelectrochemical properties; the 1.8-μm-thick film showed the highest photocatalytic activity [9]. TiO_2 nanorods of length reaching 9.8 μm were prepared by hydrothermal synthesis, but the photocatalytic activity of the films prepared from them was low because of low ability for electron transfer and low mobility of charge carriers [10], despite an increase in their active surface

area. The influence of the synthesis conditions on the nanorod behavior was studied [11]. The temperature of the hydrothermal synthesis of TiO_2 nanorods influences the degradation of anionic (Congo Red, Sirius Red) and cationic (Rhodamine B, Malachite Green) dyes. Low recombination rate and effective charge separation, ensuring higher photocatalytic performance, were reached for the TiO_2 film prepared at 140°C [12].

Up to now, no clear relationship was revealed between the nanorod geometry, specific surface area, and hydrothermal synthesis temperature; the influence of the synthesis conditions on the photocatalytic activity is not clearly understood either.

This study was aimed at determining how the hydrothermal synthesis conditions influence the photocatalytic activity of films formed by titanium dioxide nanorods.

EXPERIMENTAL

Nanostructured films based on TiO_2 nanorods were prepared in a stainless steel autoclave with a Teflon insert. The 50-mL Teflon insert was charged with a solution containing 15 mL of deionized water, 15 mL of HCl (36.5%, catalog no. 320331, Sigma–Aldrich), and 0.25 mL of titanium butylate $C_{16}H_{36}O_4Ti$ (97%, catalog no. 244112, Sigma–Aldrich). TiO_2 nanorods were synthesized on FTO supports (7 Ω cm^{-2}, catalog no. 735167, Sigma–Aldrich) preliminarily cleaned by ultrasonic treatment in a mixture of water, acetone, and 2-propanol (volume ratio 1 : 1 : 1) for 30 min. After that, the pretreated FTO supports were placed in the autoclave conducting side down. The heat treatment was performed in a convective furnace (8.2/1100, SNOL). To obtain films with different morphology, we varied the furnace temperature (100–200°C) and synthesis time (6–24 h). The samples obtained were washed with deionized water and dried at room temperature. After that, the samples were calcined at 500°C for 2 h in air.

The phase composition of the samples were determined by X-ray diffraction with an STOE STADI-P automatic powder diffractometer (STOE & Cie GmbH), Cu_{K_α} radiation, $\lambda = 1.54056$ Å, in the Bragg–Brentano geometry in the angle range 2θ 5°–80° with a step of 0.02° and counting time in each point of 5 s. The X-ray diffraction patterns were analyzed using PDF-2 powder diffraction database and built-in WinXPow program package.

The sample surface images were taken with a MIRA 3LMU (Tescan) scanning electron microscope (SEM). The accelerating electrode voltage was 20 kV. The samples were also examined by transmission electron microscopy (TEM) with a JEOL JEM 2100 F-Cs device equipped with an analyzer of the electron energy loss spectra and a spherical aberration corrector. The samples were prepared for analysis by dispersing a weighed portion (1 mg) in water under the action of ultrasound for 15 min, after which the suspension drop was applied onto copper grid (no. 01800, PELCO® TEM).

Spectrophotometric measurements were performed with a Solar CM 2203 automatic scanning calorimeter (Solar) in the wavelength range 250–800 nm with the spectrum resolution of 0.5 nm. The band gap of the TiO_2 samples was estimated from the absorption spectra of the TiO_2 nanorods with the aid of the Kubelka–Munk transformation using the formula

$$F(R) = \frac{(1-R)^2}{2R},$$

where R is the measured diffuse reflectance coefficient. The band gap width was determined as the intersection point of the linear portions of the plot of $\sqrt{F(h\nu)^2} \times 10$ vs. photon energy $h\nu$. To determine the surface area of titanium dioxide nanorod films, we determined the concentration of the adsorbed dye molecules from the absorption spectra using the formula

$$c = \frac{N_A c' V}{S}(1 - D_2 / D_1),$$

where N_A is the Avogadro number; c', concentration of dye molecules in solution; V, solution volume; S, adsorbent surface area; and D_1 and D_2, solution optical densities before and after the sorption.

To study the photocatalytic activity of the films, we measured the photoinduced current and the photodegradation of Methylene Blue dye.

The photocurrent in nanostructures from the illuminated area of 1 cm^2 was measured at a constant potential of 0 V with a potentiostat (R-20KhV, Elins, Russia) using the standard three-electrode scheme. TiO_2 nanorods were used as a working electrode; platinum foil, as an auxiliary electrode; and silver chloride electrode, as a reference electrode. Measurements were performed in 0.1 M NaOH in a specially fabricated
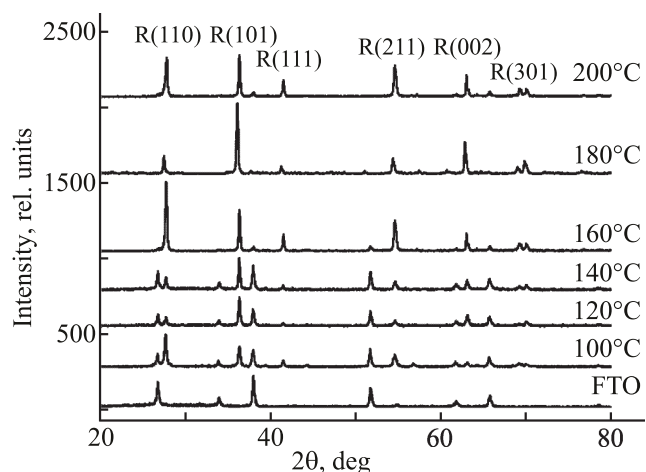
Fig. 1. X-ray diffraction patterns of TiO_2 samples prepared at different temperatures of hydrothermal synthesis.

photoelectrochemical cell with a quartz window. The photocurrent was recorded while irradiating tin dioxide films with a xenon lamp (45 mW cm^{-2}).

The photoactivity of the films formed by TiO_2 nanorods was evaluated in photodegradation of an aqueous solution of Methylene Blue dye. Plates of 1×2 cm size were immersed in 50 mL of a Methylene Blue solution (initial concentration 10^{-5} M) loaded into a quartz reactor and kept there for 20 h. After that, the spent solution was replaced by a fresh 10^{-5} M Methylene Blue solution. This procedure eliminates the errors of measuring the dye optical density, associated with the adsorption of dye molecules in the pores. The solution was continuously stirred with a magnetic stirrer. The system was irradiated with a xenon lamp (45 mW cm^{-2}). The experiment was performed for 4.5 h; the photometric measurements were made at 30-min intervals, and the dye concentration was determined from the optical density at a wavelength of 667 nm.

RESULTS AND DISCUSSION

In the diffraction pattern (Fig. 1), the major reflections belong to the tetragonal modification of TiO_2 (rutile) at 27.4°, 36.1°, 41.3°, 54.4°, 62.9°, and 69.9° and are characterized by Miller indices (110), (101), (111), (211), (002), and (301), respectively (JCPDS, no. 21–1276, $a = b = 0.4517$ nm, $c = 0.2940$ nm).

The reflections of FTO supports are observed at 2θ 26.1°, 33.96°, 37.96°, 51.76°, 61.76°, and 65.76° (JCPDS no. 18–1387). Relatively high intensities and small half-widths of the reflections show that the films are highly crystalline. With an increase in the synthesis temperature, the intensity of the diffraction maxima with indices (002) and (101) considerably increases. This fact indicates that the deposited film is highly oriented relative to the support surface. A sharp decrease in the intensity of the (110), (211), and (111) reflections also indicates that the deposited film is strongly oriented relative to the support surface; it shows that the TiO_2 nanorods grow in the [001] direction. A decrease in the intensity of the diffraction peaks corresponding to FTO supports down to the background level is apparently associated with an increase in the film thickness. In particular, the reflections corresponding to FTO supports are virtually lacking in the diffraction patterns of the films prepared at hydrothermal synthesis temperatures of 180 and 200°C.

With an increase in the synthesis time at temperatures lower than 100°C, no growth of the nanorods on the surface of FTO supports was observed. The nanorods were formed only after 3-h treatment at 100°C. The mean length of the nanorods disoriented relative to the support surface was ~120 nm in this case, and the mean nanorod diameter was ~43 nm (Fig. 2).

With an increase in the synthesis time to 24 h, the mean length of the nanorods increased to 350 nm, but their diameter remained unchanged. An increase in the temperature and time of the hydrothermal synthesis led to a considerable increase in the nanorod length and diameter. For example, at a synthesis time of 24 h, the mean nanorod length was 647, 1590, 2100, 4100, and 3200 nm for films prepared at 120, 140, 160, 180, and 200°C, respectively. Synthesis of each sample was repeated no less than 5 times, and reproducible results were obtained. Further increase in the synthesis time led to the film peeling-off from the support with the preservation of its structure. This may be due to competition between the crystal growth and dissolution. At a short synthesis time, the solution is saturated with the titanium salt, and the crystal growth prevails. With an increase in the synthesis time, the salt concentration in the solution decreases, and starting from a certain moment the crystal dissolution from the surface starts to prevail, especially at the FTO–TiO_2 interface because of
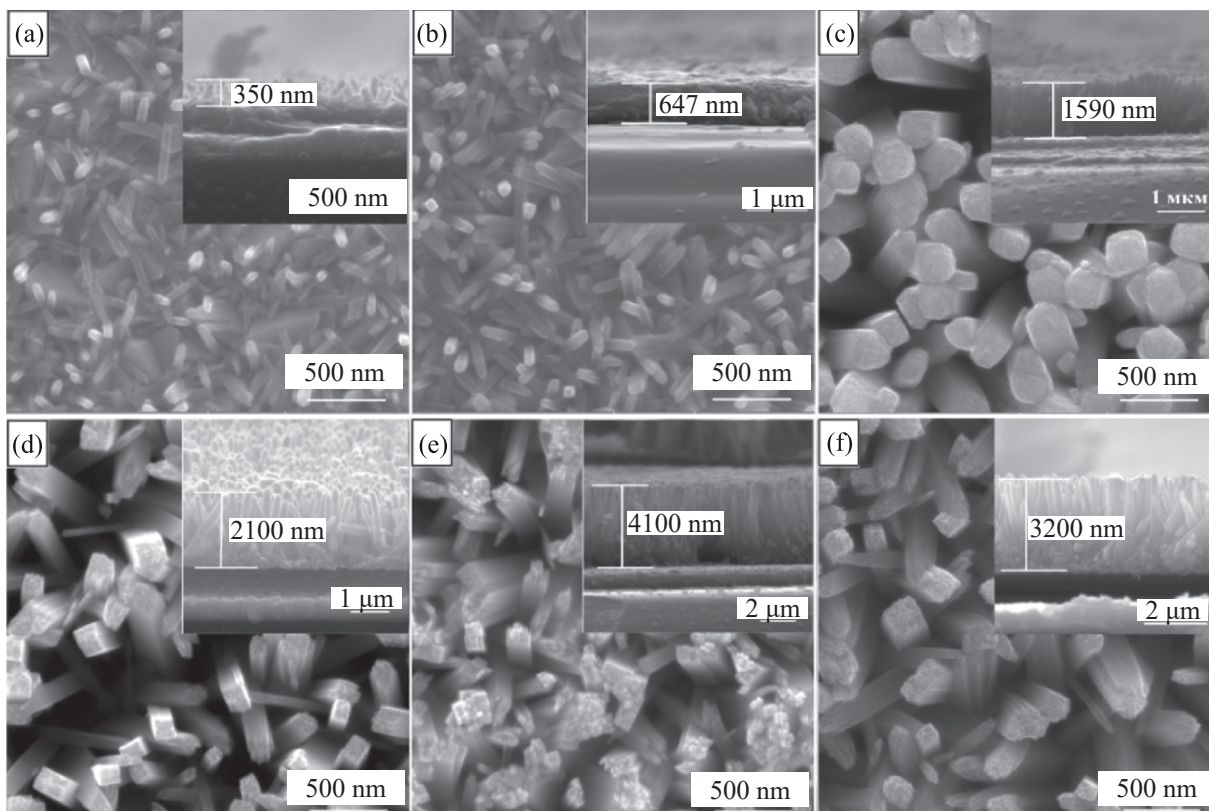
Fig. 2. Surface morphology and transverse chip of TiO$_2$ nanorods prepared at (a) 100, (b) 120, (c) 140, (d) 160, (e) 180, and (f) 200°C. Synthesis time 24 h.

differences in the crystal structures of the phases. After peeling-off of the TiO$_2$ film, the support surface remains conducting. The nanorod diameter also changes with an increase in the hydrothermal synthesis temperature. For example, the nanorod diameter was 55, 175, 120, 100, and 125 nm for the films prepared at 120, 140, 160, 180, and 200°C, respectively.

The rods ~100 nm in diameter, forming the film, consist of joined nanorods with the external diameter of ~10 nm (Fig. 3). Presumably, the initially disoriented and geometrically anisotropic crystals acquire the same growth direction, increase in the length, and densely contact with each other with an increase in the temperature and time of the hydrothermal synthesis and, correspondingly, in the autoclave pressure.

Evaluation of the photocatalytic activity of the samples by the photocurrent response and dye degradation shows that the photocurrent density in the samples sharply increased under the action of radiation and decreased without it (Fig. 4). All the samples were stable throughout the photopeak recording time.

The film prepared at the hydrothermal synthesis temperature of 180°C exhibits considerably higher photopeak intensity compared to the other samples, which, in turn, should lead to high catalytic activity,
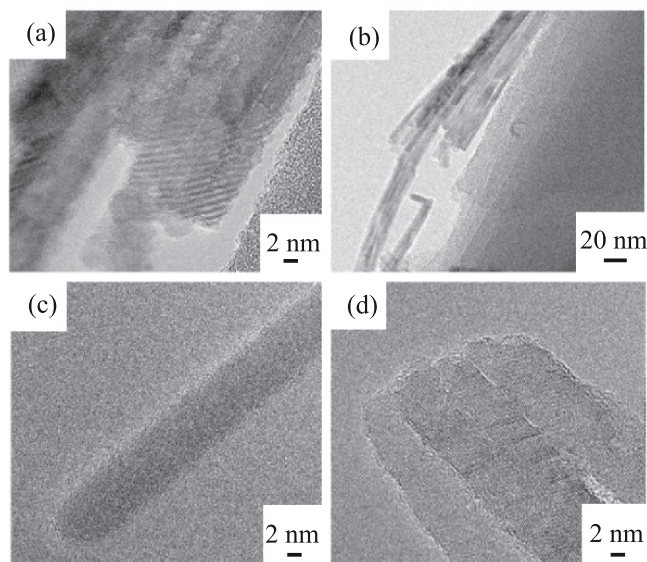

Fig. 3. Images of TiO$_2$ nanorods prepared at 180°C. (a, b) Transverse cleavage of the rod, (c) image of one rod; (d) top of the rod.
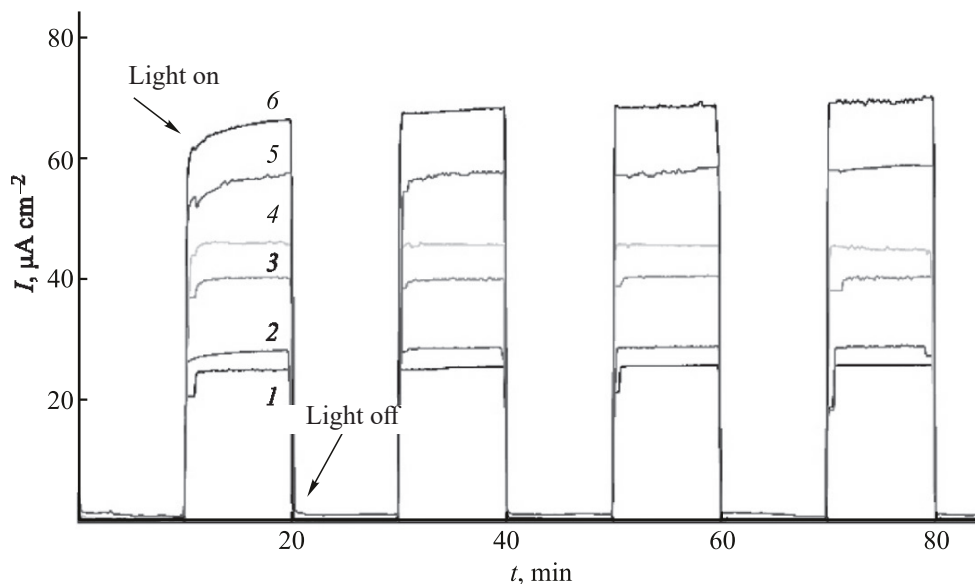
Fig. 4. Photocurrent responses of films of TiO$_2$ nanorods under simulated solar illumination. T, °C: (*1*) 100, (*2*) 120, (*3*) 140, (*4*) 160, (*5*) 200, and (*6*) 180.

because the more electrons are generated, the more efficient will be the reactions (water decomposition, degradation of dyes or other substances) in the electrochemical cell.

The photoactivity of films formed by TiO$_2$ nanorods was evaluated in experiments on photodegradation of an aqueous solution of Methylene Blue in the presence of films obtained at different temperatures of the hydrothermal synthesis (Fig. 5). The Methylene Blue

dye whose degradation under the action of TiO$_2$ has been extensively studied is used in this study as a model substrate for evaluating the photocatalyst performance [13].

The optical density of the dye decreases with an increase in the illumination time when the solution contains a TiO$_2$ film, whereas without TiO$_2$ film the optical density decreases insignificantly; i.e., the dye is quite stable under irradiation for the tested time
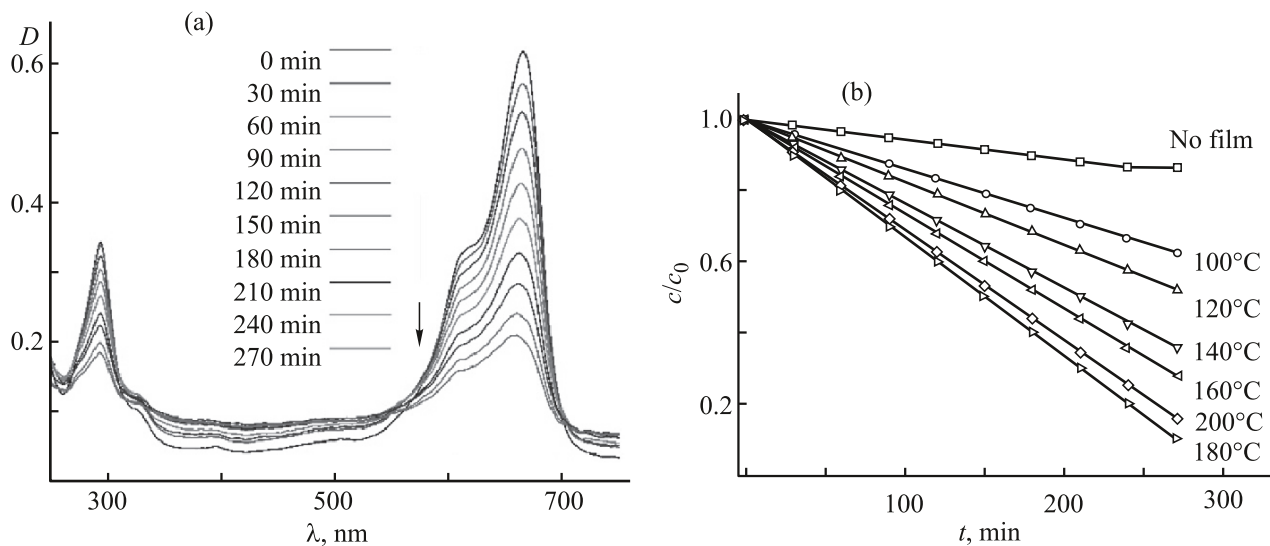

Fig. 5. (a) Absorption spectra of Methylene Blue and (b) its photodegradation in the presence of films formed by TiO$_2$ nanorods.
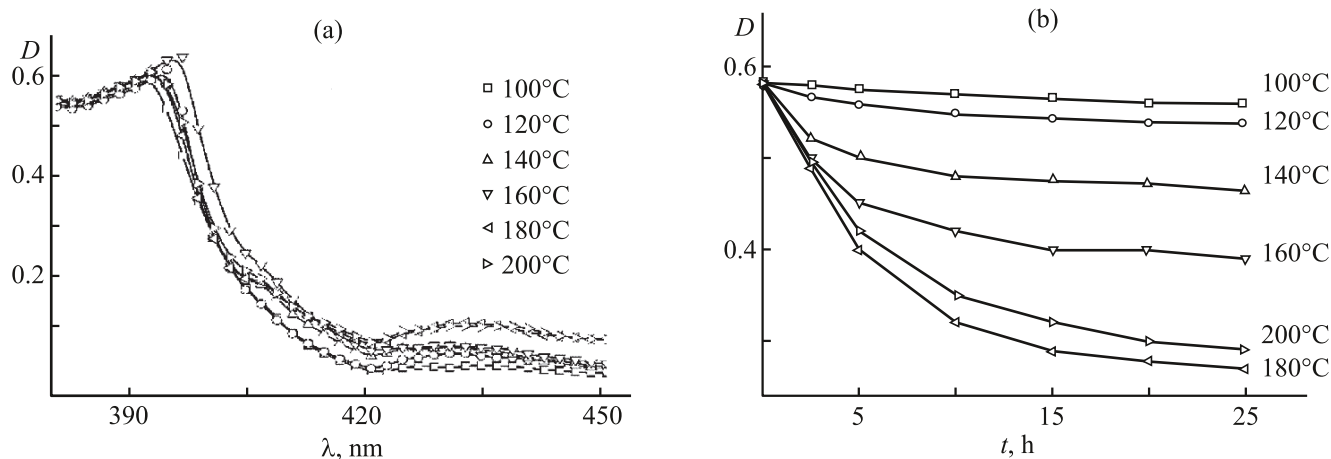
Fig. 6. (a) Absorption spectra of TiO$_2$ films and (b) dependence of the optical density of Methylene Blue dye on the sorption time.

intervals. Considerable degradation of Methylene Blue dye was observed only in the presence of a film formed by TiO$_2$ nanorods. With an increase in the hydrothermal synthesis temperature, the dye degradation rate increases. The degree of the dye degradation in 270 min in the presence of the films prepared at 180 and 200°C reached 90 and 80%, respectively, whereas the degree of the dye degradation in the same time period in the presence of the TiO$_2$ film prepared at 100°C was as low as 40%. The degree of the dye degradation in solutions with the films prepared at 120, 140, and 160°C was 53, 60, and 65%, respectively. The observed trend may be due both to changes in the optical and electrical properties of the films formed by TiO$_2$ nanorods and by changes in the active surface area. Analysis of the absorption spectra of the films formed by TiO$_2$ nanorods shows (Fig. 6a) that the band gap width varies insignificantly and is 3.05–3.07 eV.

Thus, the effect of the TiO$_2$ band gap width on its photocatalytic activity can be neglected. The photocatalytic activity of the samples may be influenced by their active surface area. Absorption of a light quantum by a superconductor in contact with a liquid leads to excitation of effective charge carriers in the bulk of the semiconductor, which are separated and participate in the cleavage reaction. In the case of heterogeneous catalysis, an increase in the active surface area of the samples favors an increase in the reaction rates.

We examined the influence of the film deposition temperature on the specific surface area of the films. TiO$_2$ nanorods are difficult to separate from the surface of FTO supports; therefore, it is impossible to estimate the specific surface area by low-temperature nitrogen porosimetry. The active surface area was estimated from the amount of the adsorbed Methylene Blue dye molecules. With an increase in the adsorption time (Fig. 6b), the optical density of the solution decreased, suggesting sorption of Methylene Blue dye molecules in pores and on the surface of the semiconductor films. The sorption onto the films prepared at 100 and 120°C was slow. The largest change in the optical density was observed for the solution in contact with the film prepared at 180°C. The decrease in the optical density and hence in the dye concentration was intense in the first 15 h, after which it decelerated. At the adsorption time of 20–25 h, the optical density of the solution did not noticeably change further, suggesting saturation of the films. From the data obtained, we calculated the amounts of Methylene Blue dye molecules adsorbed in pores and on the surface of semiconductor TiO$_2$ films (Table 1).

Assuming that the area occupied by one Methylene Blue dye molecule is 130 Å^2 [14], we obtain for the surface area of the film synthesized at 180°C (film with the largest surface area) the value of 6.2 × 10^{17} Å^2, or ~62 cm^2 per 1 cm^2 of the film of TiO$_2$ nanorods deposited on the support surface. The results obtained allow a conclusion that the photocatalytic activity of TiO$_2$ nanorods prepared at different temperatures of the hydrothermal synthesis depends on the active surface area of the films. The film of TiO$_2$ nanorods synthesized at 180°C has the largest active surface area and exhibits

Table 1. Results of evaluating the sorption capacity of semiconductor films formed by TiO_2 nanorods

Hydrothermal synthesis temperature, °C	Amount of molecules, molecule cm^{-2}	Occupied area, $Å^2$
100	2.7×10^{14}	3.5×10^{16}
120	5.4×10^{14}	7.0×10^{16}
140	1.8×10^{15}	2.3×10^{17}
160	2.7×10^{15}	3.5×10^{17}
180	4.8×10^{15}	6.2×10^{17}
200	4.3×10^{15}	5.5×10^{17}

the maximal photocatalytic activity compared to the other films.

CONCLUSION

Variation of the temperature (100, 120, 140, 160, 180, 200°C) and time of the hydrothermal synthesis leads to the formation on FTO supports of TiO_2 nanorods with the rod length of 350, 647, 1590, 2100, 4100, and 3200 nm and mean diameter from 55 to 125 nm, respectively. The film formed by TiO_2 nanorods, prepared by the 24-h synthesis at 180°C, exhibits the highest photocatalytic activity. The optical density of the films and the semiconductor band gap width varied insignificantly with the synthesis temperature; therefore, the effect of these parameters on the photocatalytic activity of the films can be ruled out. An increase in the hydrothermal synthesis temperature led to an increase in the film crystallinity; the optimum length and diameter of TiO_2 nanorods were found for ensuring high specific surface area and high catalytic activity of the films.

CONFLICT OF INTEREST

The authors declare that they have no conflict of interest.

REFERENCES

1. Lazar, M.A., Varghese, S., and Nair, S.S., *Catalysts,* 2012, vol. 2, no. 4, pp. 572–601.
https://doi.org/10.3390/catal2040572

2. Zhao, Y., Hoivik, N., and Wang, K.Y., *Nano Energy,* 2016, vol. 30, pp. 728–744.
https://doi.org/10.1016/j.nanoen.2016.09.027

3. Serikov, T.M., Ibrayev, N.K., Nuraje, N., Savilov, S.V., and Lunin, V.V., *Russ. Chem. Bull.,* 2017, vol. 66, no. 4, pp. 614–621.
https://doi.org/10.1007/s11172-017-1781-0

4. Wang, F.Y., Song, L.F., and Zhang, H.C., *J. Electron. Mater.,* 2017, vol. 46, no. 8, pp. 4716–4724.
https://doi.org/10.1007/s11664-017-5491-z

5. Serikov, T.M., Ibrayev, N.K., and Smagulov, Z., *IOP Conf. Ser. Mater. Sci. Eng.,* 2016, vol. 110, ID 012066.
https://doi.org/10.1088/1757-899X/110/1/012066

6. Yamazaki, Y., Fujitsuka, M., and Yamazaki, S., *ACS Appl. Nano Mater.,* 2019, vol. 2, pp. 5890−5899.
https://doi.org/10.1021/acsanm.9b01334

7. Liu, B., Boercker, J.E., and Aydil, E.S., *Nanotechnology,* 2008, vol. 19, no. 50, pp. 505604–505609.
https://doi.org/10.1088/0957-4484/19/50/505604

8. Yamazaki, Y., Azami, K., Katoh, R., and Yamazaki, S., *ACS Appl. Nano Mater.,* 2018, vol. 10, pp. 5927–5935.
https://doi.org/10.1021/acsanm.8b01617

9. Hwang, Y.J., Hahn, C., Liu, B., and Yang, P., *ACS Nano,* 2012, vol. 6, no. 6, pp. 5060–5069.
https://doi.org/10.1021/nn300679d

10. Kerkez, Ö. and Boz, I., *React. Kinet. Mech. Catal.,* 2013, vol. 110, pp. 543–557.
https://doi.org/10.1007/s11144-013-0616-8

11. Liu, B. and Aydil, E.S., *J. Am. Chem. Soc.,* 2009, vol. 131, no. 11, pp. 3985–3990.
https://doi.org/10.1021/ja8078972

12. Ravidhas, C., Anitha, B., Arivukarasan, D., Venkatesh, R., Christy, A.J., Jothivenkatachalam, K., and Sanjeeviraja, C., *J. Mater. Sci.: Mater. Electron.,* 2016, vol. 27, no. 5, pp. 5020–5032.
https://doi.org/10.1007/s10854-016-4389-5

13. Kwon, C.H., Shin, H.M., Kim, J.H., Choi, W.S., and Yoon, K.H., *Mater. Chem. Phys.,* 2004, vol. 86, no. 1, pp. 78–82.
https://doi.org/10.1016/j.matchemphys.2004.02.024

14. Kahr, G. and Madsen, F.T., *Appl. Clay Sci.,* 1995, vol. 9, no. 5, pp. 327–336.
https://doi.org/10.1016/0169-1317(94)00028-o